



CHEMOPREVENTIVE EFFICACY OF HONOKIOL ON EXPERIMENTALLY INDUCED HAMSTER BUCCAL POUCH SQUAMOUS CELL CARCINOMA

Sanad A. Mosbah^{1*}, Mahmoud A. Elsayed², Ahmed Abd-Alshakor Abd-Alhafez³, Mohamed Gomaa Attia-Zouair⁴

ABSTRACT

Abstract: The aim of the present study was to investigate the effect of honokiol on induced hamster buccal pouch (HBP) squamous cell carcinoma (SCC). **Subjects and methods:** Thirty hamsters were used and divided into three groups (G_s), 10 each. G_I (normal) was left untreated, the right HBP in G_{II} were painted with 0.5% DMBA (3times/week/14weeks). G_{III} was treated as G_{II}, in addition, they received honokiol. After termination of experiment, the hamsters were clinically examined, then, euthanized. After that, HBP was excised and routinely prepared for histological examination using hematoxylin and eosin (H&E) stain to record the histopathological findings and the depth of invasion, and histochemically examination utilizing AgNOR stain and picosires red stain as proliferative and invasive marker respectively, to record the mean area percentages for statistical analysis. **Results:** Gross and histopathological observations revealed variable changes in G_{III} compared to G_{II}. The statistical analysis results, for the depth of invasion, revealed high significant difference between G_{II} and G_{III}, with p-value:<0.001. Regarding the AgNOR stain, there was high significant difference between G_I and G_{II} and, also, between G_{II} and G_{III} with p-value: <0.001. The polarizing colors of collagen fibers recorded significant difference between G_I and G_{II}, G_I and G_{III}, G_{II} and G_{III} with p-values: 0.042, 0.200, and: 0.175 respectively. The area fraction of the collagen fibers recorded high significant difference between G_I and G_{II} and, also, between G_{II} and G_{III} with p-values: <0.001 for both. **Conclusions:** Honokiol significantly inhibited of invasion, proliferative activity and tumor progression in DMBA induced HBP SCCS.

KEYWORDS: HBP squamous cell carcinoma, Honokiol, Chemoprevention.

INTRODUCTION

Conventional oral squamous cell carcinoma (OSCC) is one of the most common cancers of the head and neck. The incidence of OSCC has increased in many countries, especially in younger age groups^(1,2). Experimental oral carcinogenesis induced by 7,12 dimethylbenz(a)anthracene (DMBA) in golden

Syrian hamster buccal pouch (HBP) was found to be an accepted and well recognized experimental model for studying biochemical, histopathological, immunohistochemical and molecular alterations in OSCC⁽³⁾. Treatment of oral caners involves surgery or radiation in combination with chemotherapy using chemicals, such as 5-Fluresen and cisplatin⁽⁴⁾.

1. Faculty of Dental Medicine, Bengazi University, Libya.

2. Lecturer Oral and Dental Pathology Department,, Faculty of Dental medicine(Boy-Cairo), AlAzhar University, Egypt

3. Lecturer, Oral and Dental Pathology Department,

4. Professor, Oral and Dental Pathology Department, Faculty of Dental Medicine (Boys-Cairo), Al-Azhar University, Egypt.

• **Corresponding author:** Sanadaltajore1991@gmail.com.

Surgical resection causes permanent disfigurement, altered sense of self, crippling physiological effects, significant cognitive disability and morbidity, although chemo and radiotherapy have substantial side effects, they both have an impact on the patient's well-being and quality of life⁽⁵⁾.

Phytochemicals are natural biologically active compounds with potential health benefits; they have become a focus in recent years. Phytochemicals have been shown to have anticancer effects, mainly by regulating epigenetics/epigenomics⁽⁶⁾. Phytochemicals can be divided into phenolic compounds, carotenoids and others. Phenolic compounds contain one (phenolic acids) or more (polyphenols) aromatic rings with attached hydroxyl groups in their structures. Phenolic acid can be classified into hydroxycinnamic acid and hydroxybenzoic acid. Hydroxycinnamic acid is found in cinnamon, coffee, blueberries, kiwis, plums, apples and cherries. However, hydroxybenzoic acid is found in few consumable plants⁽⁷⁾.

Honokiol ($C_{18}H_{18}O_2$) is a natural biphenolic compound extracted from the leaves and barks of *Magnolia officinalis* and is widely used in traditional Chinese medicine. Honokiol has been reported to have several pharmacological effects, including anti-inflammation, anti-aging, anti-bacterial, neuroprotective, anti-oxidant and anti-cancer effects^(8,9).

The tumor mass growth rate is one of the most important factors influencing the clinical outcome of cancer and faster growth is suggested to explain the worse prognosis of cancers⁽¹⁰⁾. Several proliferative markers have been developed to assess proliferative index and for that matter aggressiveness and grade of the tumor as well as the survival chances. One of these markers is argyrophilic nuclear organizer region (AgNOR) was found to be more abundant in malignant cells than in benign neoplastic cells and was also used initially as a parameter for the diagnosis of malignancy. This technique involves silver staining of a peculiar group of highly

argyrophilic acidic proteins present in Nuclear Organizer Regions (NORs), thus allowing NORs to be clearly and selectively visualized at the light microscopic level by specific silver nitrate staining procedure⁽¹¹⁾.

Moreover, it is well known that collagenous stroma plays a very important role in inhibiting spread of the malignant tumor cells by acting as a barrier. However, in malignancies there occurs stromal remodeling which weakens the stroma to facilitate the spread of the tumor^(12,13). Depth of invasion (DOI) is defined as a measurement from the basement membrane zone to the deepest point of cancer cell invasion⁽¹⁴⁾. In the recent 8th edition of the American Joint Committee on Cancer (AJCC) classification, depth of invasion has been added into the TNM staging of the tumor to improve its prognostic value⁽¹⁵⁾. It has been found that picosirius red stain is the special method, used to study the nature of the collagen fibers by using its birefringence properties⁽¹⁶⁾. The change in birefringence of collagen fibers surrounding the tumor islands with increasing grade of the tumor is highlighted under polarized microscope stained with picosirius red stain; as stroma changes from red-yellow to green when the grade of tumor increases. The changes in the stromal birefringence are attributed to the change from mature collagen fibers to immature⁽¹⁷⁾. In this regard, the present study was carried out to investigate the effect of honokiol as a new chemopreventive modality in experimentally induced HBP SCC. The assessment was based on the gross observation, histologically examination utilizing hematoxylin and eosin (H&E) stain to record the histopathological findings and the DOI, and histochemically examination utilizing (Ag-NOR) stain and picosirius red stain as proliferative and invasive marker respectively.

MATERIAL AND METHODS

The experimental animal models included thirty golden Syrian male hamsters, five weeks old, weighing 80-120 gm, were obtained from the

animal house, Cairo University (Cairo, Egypt). The animals were housed in show box cages at the Private Experimental Animal Unit belong to specialists working at the Faculty of Pharmacy, Boys, Cairo, Egypt, Al-Azhar University. The controlled environment was maintained under standard conditions. The hamsters were fed and watered ad-libitum in accordance to the guidelines of the medical research institute, international guiding principles for biomedical research involving animals⁽¹⁸⁾.

Sample size:

Based on Kullage et al (2017)⁽¹⁹⁾ research, a sample size of 10 animals in each group, in the current study, were have a 80% power to detect a difference between means of 0.53 with a significance level (alpha) of 0.05 (two-tailed) at 95% confidence intervals. In 80% (the power) of those experiments, the p value was less than 0.05 (two-tailed) so the results were deemed “statistically significant”. In the remaining 20% of the experiments, the difference between means was deemed “not statistically significant”. Report created by Graph Pad Stat Mate 2.00.

Experimental design:

After one week of adaptation, the animals were divided into three group_(s) (G_(s)), 10 each. While the hamsters in GI (normal) were, left untreated, the right HBP in GII (DMBA treated group), were painted with carcinogen 0.5% DMBA (Sigma-Aldrich) 3 times a week, for 14 weeks, using a number 4 camel’s hair brush⁽²⁰⁾. Whereas the hamsters in GIII (honokiol chemoprevention group) were treated as in GII, in addition, they received intra-peritoneal 10 mg/kg honokiol dissolved in normal saline using insulin syringe⁽²¹⁾, a week before, as well as, during the application of DMBA on alternative days. After the termination of the experiment, the clinical examination of hamsters in all groups were done to record the alterations that may be happened throughout the experiment

(healthy hamsters displayed sign such as normal, smooth gait, bright, clear eyes, healthy skin (on their ear, too), good coat that is free of dry patches parasites, and buccal mucosa appeared healthy without any cuts or scabs. Diseased hamsters exhibiting sings such as inactive, loss of appetite, hiding in corner, ruffled or unkempt coat, sneezing, wheezing and/or discharged from the nose or eyes, diarrhea (causing wetness around the tail), hair loss (often sign of parasites or allergies), then, the hamsters were euthanized and their buccal pouches were excised in order to be prepared.

Preparation and investigations:

The tissue sections were fixed in 10% neutral buffered formalin at room temperature for 24 hours, routinely processed and embedded in paraffin blocks for sectioning and preparation in order to be stained. For staining procedures, tissue sections were cut at 4 μ m thick and routinely processed to be stained with H&E stain for recording the histopathological findings. After that, the DOI was reviewed and measured according to the AJCC 8th classification. The measurement was taken from the level of the basement membrane of the closest adjacent normal mucosa. A vertical line was drawn from this plane to the deepest point of tumor invasion⁽²²⁾.

For AgNOR staining method:

AgNOR staining was carried out by standard staining method⁽²³⁾. The tissue Sections of 4- μ m thickness were cut from the routinely prepared paraffin blokes and put on glass slides. The sections were, then, dewaxed in three changes of xylene and after that hydrated through diving evaluations of liquor to refined water. The fresh prepared AgNOR stain arrangement was readied and quickly poured over the tissue specmints and left for 40 minutes, at 370°C temperature in the incubator. After staining was done, the slides were washed in deionized water. The sections were deparaffinized, rehydrated and then washed in running de-ionized water for 10 minutes. The tissue section were then stained with

silver colloidal solution freshly prepared by mixing one part of 2% gelatine in 1% aqueous formic acid and two parts of 50% silver nitrate and incubated in the dark at 30°C for 45 minutes. The sections were then washed in running de-ionized water, dehydrated, cleared and mounted in synthetic resin medium. AgNORs were seen as distinct intranuclear black dots and were randomly counted manually in 50-100 nuclei under $\times 1000$ magnification with oil immersion lens and recorded on an MS Excel sheet⁽²⁴⁾.

For picrosiures red staining procedures:

Picrosiures red stain staining was carried out by standard staining method⁽²⁵⁾. The tissue sections were cut at 4 μ m thickness and mounted on positive charged glass slides. The Slides were deparaffinized and rehydrated through distilled water. The sections were incubated in hematoxylin (H-3404; Vector Laboratories, Inc, Burlingame, CA) for 8 minute then washed in running tap water for 10 minutes. The Slides were incubated for 1 hr at 25C in the PSR staining solution [0.5 g of Direct Red 80 (2610-10-8; Sigma-Aldrich Corp., St. Louis, MO) in 500 mL of saturated picric acid (P6744-1GA; Sigma-Aldrich Corp.)]. Slides were washed in two change of acidified water (0.5% acetic acid), then dehydrated in three change of 100% isoprpyl alcohol for 1 minute each. Slides were cleared in xylene and mounting in DPX (resinousmedia). The slides were then examined in detail under polarized microscope (Olympus BX 41), to analyze the polarizing colors of the collagen fibers. Nature of collagen was analyzed in five random high power fields at 400x magnification the findings were recorded. Based on color observed, nature of collagen was recorded as three categories as proposed by Venigella and Charu (red-orange, yellow-orange, or green/greenish-yellow)⁽²⁶⁾. After that the images of PSR at 400x magnification were fed into computer image analysis software (OLYMPUS stream image analysis software, version 1.47), and the percentage of area occupied by collagen fibers in a given field was calculated⁽²⁷⁾.

Statistical analysis:

The data: (mean, standard deviations and range) was recorded and statistically analyzed. The comparison between more than two independent groups with quantitative data and parametric distribution was done by using **One Way ANOVA**. In addition, **Tukeys post hoc test** was performed when ANOVA test reveals significant difference (p value > 0.05: Non significant (NS), p value < 0.05: Significant (S) and p value < 0.01: Highly significant (HS)), and to determine the correlation between the proliferation and invasion.

RESULTS

Gross observation findings:

The gross observation, the histopathological feature using: H& E stain, AgNOR stain and picrosiures red stain as well as the statistical analysis results among the various groups examined were shown in Figs.1-14, and Tables 1-3 as well as in Figs 15-17.

The gross observation results (**Table 1**): The gross observation result in GI, all hamsters appeared active and healthy. The right HBP mucosa showed normal mucosa with pink color and smooth surface (**Fig. 1**). In GII, all hamsters showed loss of activity and also debilitation. The right HBP mucosa revealed variable changes. 7 hamsters out of 10 showed large exophytic nodules with ulcerative areas (**Fig. 2**). The other 3 hamsters showed relatively large exophytic masses, compared to those seen in the first 7 ones, surrounding with ulceration and bleeding areas. In GIII, 6 hamsters out of 10 appeared almost healthy and active, the other 4 appeared loss of activity and also debilitation. The right HBP mucosa revealed variable changes. 3 hamsters out of 10 exhibited small tiny elevations with an absence of ulcerations and bleedings, 3 hamsters had white grayish erythematous mucosal surface, while 4 hamsters had a relatively small exophytic nodules (**Fig. 3**).

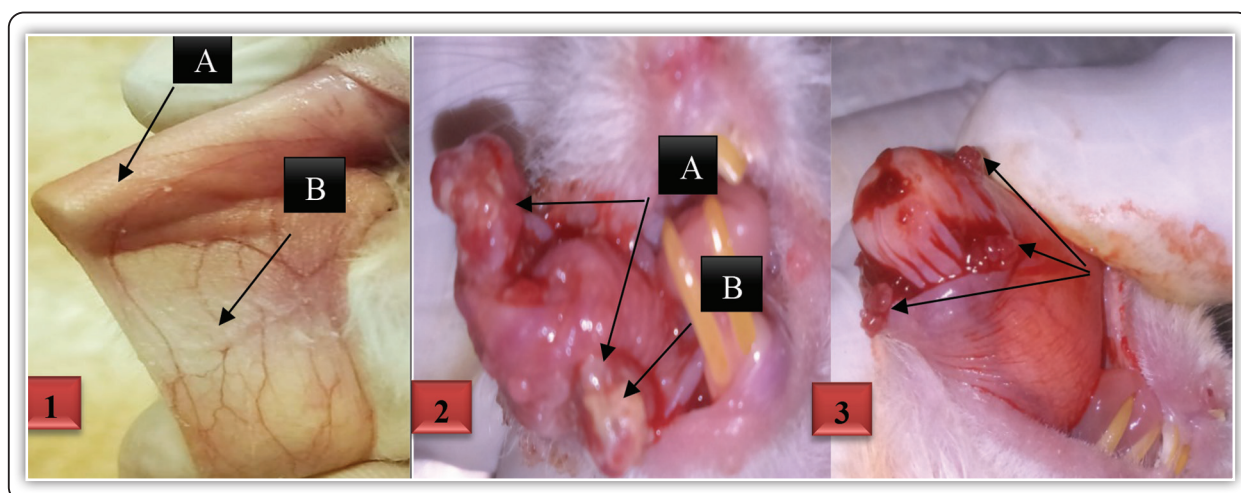


FIG (1): HBP mucosa in GI showed normal mucosa with pink color (A), and smooth surface (B). **FIG (2):** HBP mucosa in GII showed large exophytic nodules (A), with ulcerative area (B). **FIG (3):** HBP mucosa in GIII showed a relatively small exophytic nodules (arrows).

Histopathological and histochemical results:

In GI, the histological tissue sections, using H&E stain, the HBP mucosa exhibited normal features of thin stratified squamous epithelium, consisting of two to four layers of squamous cells with slight keratinization (i.e.; one layer of basal cells, one two or three layers of spinous cells and thin keratinized cells with lacking rete ridges. Subepithelial connective tissue, and muscular layer were seen (Fig. 4). Using AgNOR stain, the epithelial cells displayed dispersed brown to black round dots, of distinct sizes with regular boundaries inside brownish nucleus within pale yellow background (Fig. 5), with mean area 2.1% (Table 1). The picosires red stain, revealed large amount of thick, densely, packed collagenous stroma (Collagen type I) which exhibited reddish-orange birefringence with mean area 90%, other areas showed relatively less amount of thin, loosely, dispersed collagenous stroma (Collagen type III) which exhibited greenish-yellow birefringence with mean area 10% (Fig. 6, Table 2).

In GII, HBP mucosa, using H&E stain, revealed variable changes. In 7 hamsters out of 10, the overlying epithelium revealed multiple areas with dysplastic features including pleomorphism, hyperchromatism and abnormal mitotic figures. Destruc-

tive basement membrane providing evidence of prominent true invasion with formation of epithelial nests and keratin pearls (well differentiated SCC) were seen (Fig. 7). In the other 3 hamsters, the overlying epithelium revealed dysplastic features accompanied destruction of the basement membrane. The underlying connective tissue contained deeply invasive nests (6.4mm) of moderately differentiated SCC. The mean DOI in GII (10 hamsters) revealed 7mm (Fig. 8, Table 1). The AgNOR stain highlighted large, black dots and/or bizarre clusters with irregular outline inside brownish nucleus within pale clear background throughout the epithelial cells (Fig. 9), with mean area 6.9%. (Table 1). The picosires red stain displayed large amount of thin, loosely, dispersed collagenous stroma (Collagen type III) which exhibited greenish-yellow birefringence with mean area 60%, other areas showed relatively less amount of displayed large amount of thick, densely, packed collagenous stroma (Collagen type I) which exhibited reddish-orange birefringence with mean area 40% (Fig. 10, Table 2).

In GIII, HBP mucosa, using H&E stain, revealed variable changes. One hamster out of 10 exhibited hyperplastic epithelium with no feature of epithelial dysplasia. 2 hamsters revealed moderate epithelial dysplasia with feature included cellular pleomorphism, hyperchromatism and basilar

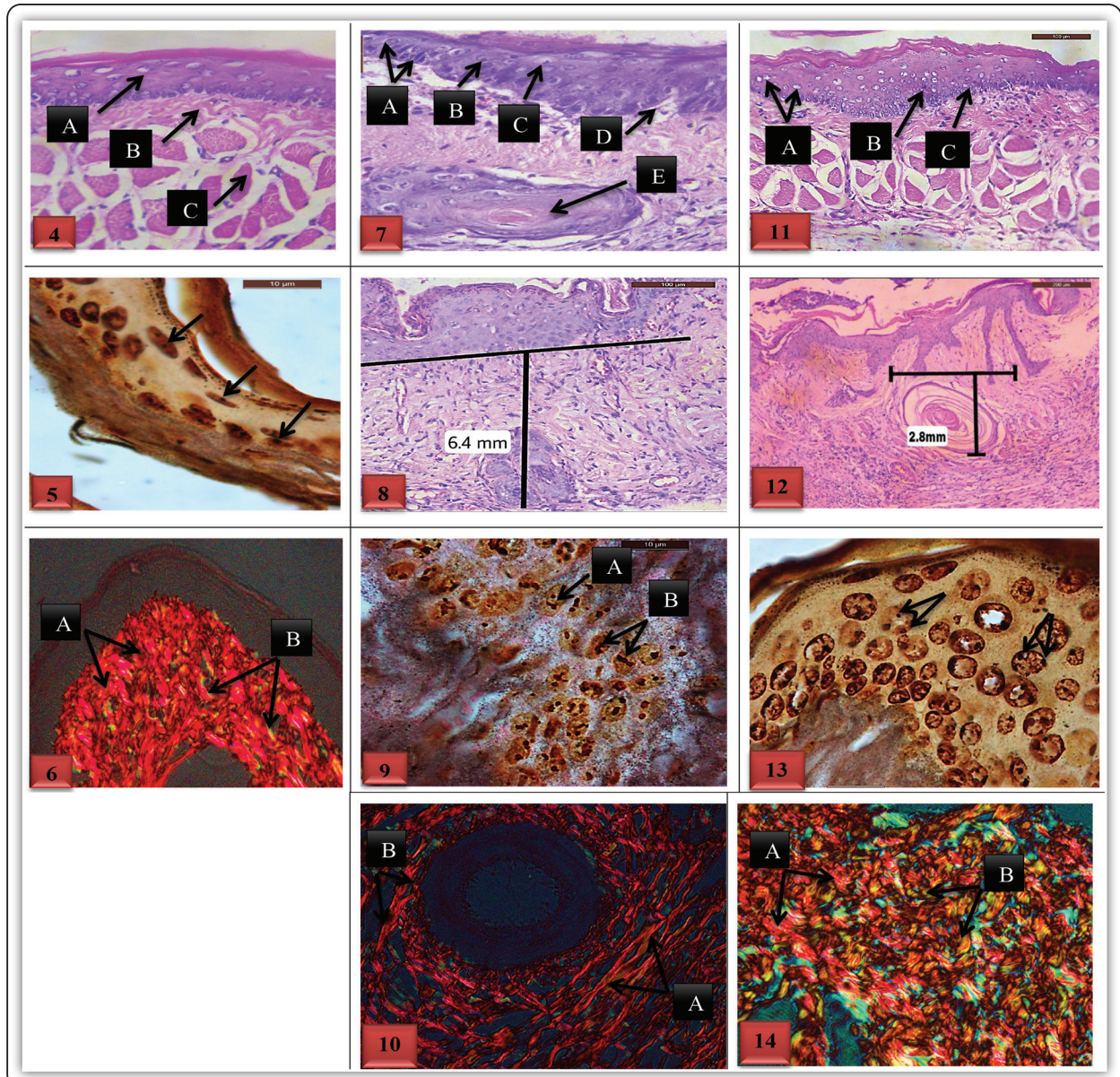


FIG. (4): HBP in GI showed thin keratinized stratified squamous epithelium consists of two to four layers with flattened rete ridges (A), subepithelial connective tissue layer (B), and muscular layer (C) (H&E stain, X200). **FIG. (5):** HBP in GI showed epithelia cells with dispersed brown to black round dots with regular boundaries within brown nucleus (arrows) (AgNOR stain, X1000). **FIG. (6):** HBP in GI showed large amount of thick densely packed collagenous stroma (Collagen type I) which exhibited reddish-orange birefringence (A), other areas showed relatively less amount of thin, loosely, dispersed collagenous stroma (Collagen type III) which exhibited greenish-yellow birefringence (B) (Picrosirius red stain, X400). **FIG. (7):** HBP in GII showed overlying epithelium with dysplastic feature including cellular pleomorphism (A), hyperchromatism (B), abnormal mitosis figure (C), and destructive basement membrane (D). The underlying connective tissue contained invasive island of neoplastic epithelia cells with keratin pearl (E) (H&E stain, X200). **FIG. (8):** HBP in GII showed deeply invasive nest of carcinoma cells (DOI=6.4mm) (H&E stain, X200). **FIG. (9):** HBP mucosa in GII showed epithelia cells with large, black dots (A) and/or bizarre clusters (B) with irregular outline within brown nucleus (AgNOR stain, X1000). **FIG. (10):** HBP mucosa in GII showed displayed large amount of thin, loosely, dispersed collagenous stroma (Collagen type III) which exhibited greenish- yellow birefringence (A), other area showed a relatively less amount thick densely packed collagenous stroma (Collagen type I) which exhibited reddish-orange birefringence (B) (Picrosirius red stain, X400). **FIG. (11):** HBP mucosa in GIII showed moderate epithelial dysplasia with cellular pleomorphism (A), hyperchromatism (B), and basilar hyperplasia (C). (H&E stain, X200). **FIG. (12):** HBP mucosa in GIII showed superficial invasive neoplastic epithelial island with keratin pearl (DOI=2.8mm) (arrow). (H&E stain, X200). **FIG. (13):** HBP mucosa in GIII showed epithelial cell with small, wider scattered, black dots with irregular outline within brown nucleus (arrows) (AgNOR stain, X1000). **FIG. (14):** HBP mucosa in GIII showed large amount of thick, densely packed collagenous stroma (Collagen type I) which exhibited reddish-orange birefringence (A), other areas showed relatively less amount of thin, loosely, dispersed collagenous stroma (Collagen type III) which exhibited greenish-yellow birefringence (B). (Picrosirius red stain, X400).

hyperplasia which extending in one-half of the epithelial thickness with intact basement membrane (**Fig. 11**), 3 hamsters displayed severe epithelial dysplasia with features included frequent mitotic figures, cellular pleomorphism, nuclear atypia, and some early disturbance of the keratin layer with drop shaped rete pigs which extending beyond one-half of the epithelial thickness but not affecting the entirety of the epithelium with intact basement membrane. In the other 4 hamsters, the overlying epithelium exhibited dysplastic features accompanied destruction of the basement membrane. The underlying connective tissue contained superficial invasive (2.8mm) epithelial nests and keratin pearl (well differentiated SCC). The mean DOI in GIII (10 hamsters) revealed 3mm (**Fig. 12, Table 1**). The AgNOR stain showed small, wider scattered black dots with irregular outline inside brownish nucleus within pale yellow back ground of the epithelial cells (**Fig. 13**), with mean area 4.2% (**Table 1**). The picosiuers red stain showed large amount of thick, densely, packed collagenous stroma (Collagen type I) which exhibited reddish-orange birefringence

with mean area 80%, other areas showed a relatively less amount of thin, loosely, dispersed collagenous stroma (Collagen type III) which exhibited greenish-yellow birefringence with mean area 20% (**Fig. 14, Table 2**).

Statistical analysis results:

Regarding the depth of invasion, the statistical analysis results revealed high significant difference between GII and GIII, with p-value:<0.001(**Table 1, Fig. 15**). Regarding AgNOR stain, the mean AgNOR dots number per nucleus recorded high significant difference between GI and GII and, also, between GII and GIII with p-value: <0.001(**Table 1, Fig. 15**). Concerning picosiuers red stain, the polarizing colors of collagen fibers recorded significant difference between GI and GII, GI and GIII, GII and GIII with p-values: 0.042, 0.200, and: 0.175 respectively (**Table 2, Fig. 16**). The area fraction of the collagen fibers recorded high significant difference between GI and GII and, also, between GII and GIII with p-values: <0.001(**Table 3, Fig. 17**).

TABLE (1) The statistical analysis results of depth of invasion and AgNOR dots number per nucleus in the study groups.

		Group I	Group II	Group III	Test value	p-value	Sig.
		No. = 10	No. = 10	No. = 10			
Depth of invasion (mm)	Mean±SD	0.00 ± 0.00	7.00 ± 1.49	3.00 ± 0.82	128.077	0.000	HS
	Range	0 – 0	5 – 9	2 – 4			
AgNOR stain	Mean±SD	2.10 ± 0.74	6.90 ± 0.74	4.20 ± 0.79	101.513•	0.000	HS
	Range	1 – 3	6 – 8	3 – 5			
Post Hoc analysis by LSD							
Parameter	Group I Vs Group II	Group I Vs Group III	Group II Vs Group III				
Depth of invasion (mm)	0.000	0.000	0.000				
AgNOR stain	0.000	0.000	0.000				

TABLE (2) The statistical analysis results of polarizing colors of collagen fibers in the study groups.

Collagen	Group I	Group II	Group III	Test value	p-value	Sig.
	No. = 10	No. = 10	No. = 10			
RO	7 (70.0%)	2 (20.0%)	3 (30.0%)	10.167*	0.038	S
YO	2 (20.0%)	2 (20.0%)	5 (50.0%)			
GY	1 (10.0%)	6 (60.0%)	2 (20.0%)			

Multi-comparison between groups		
Group I Vs group II	Group I Vs group III	Group II Vs group III
0.042	0.200	0.175

OR: orange-red. YO: yellow-orange. GY: green-yellow.

TABLE (3) The statistical analysis results of area fraction of collagen fibers in the study groups.

Area fraction of collagen fiber	Group I	Group II	Group III	Test value	p-value	Sig.
	No. = 10	No. = 10	No. = 10			
Mean ± SD	43.8 ± 1.69	15.4 ± 2.88	27.4 ± 4.25	209.140	0.000	HS
Range	41 – 46	13 – 20	23 – 35			

Post Hoc analysis by LSD		
Group I Vs Group II	Group I Vs Group III	Group II Vs Group III
0.000	0.000	0.000

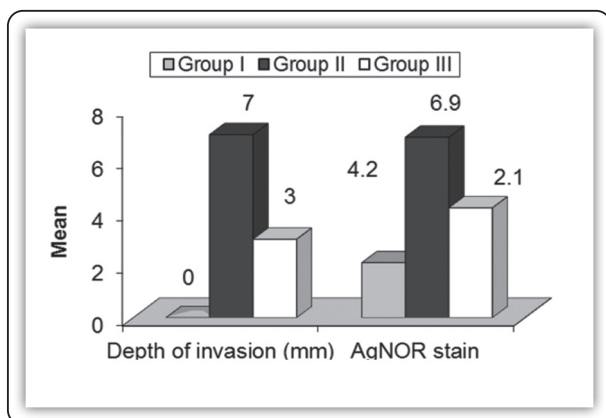


FIG (15) Bar chart representing mean depth of invasion (by mm) and mean area % results of AgNOR dots number per nucleus in the study groups.

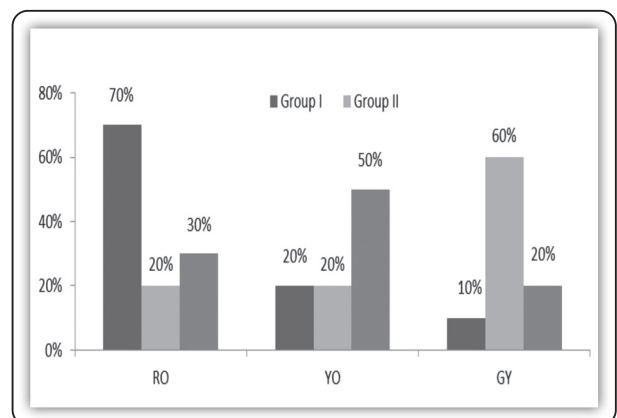


FIG (16) Bar chart representing mean area % results of polarizing colors of collagen fibers in the study groups.

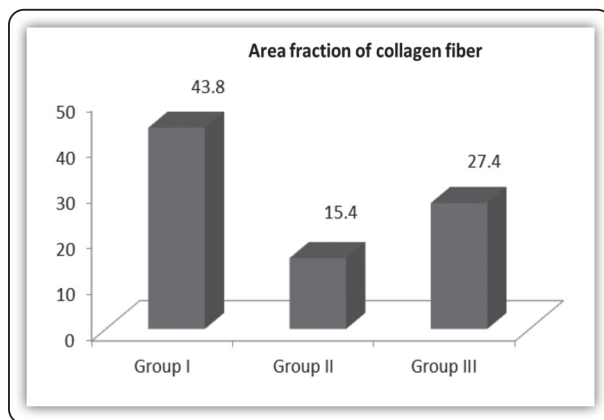


FIG (17) Bar chart representing mean area % results of fraction of collagen fiber in the study groups.

DISCUSSION

Oral carcinogenesis is a highly complex process which takes place when squamous epithelium is affected by multiple genetic and environmental alterations. As a matter of interest, the challenge directed not only toward the treatment, but also toward early detection or even to prevent the progression of this process using various chemopreventive modalities.

In this regard, the results of the present study successfully revealed the effect of honokiol as a new chemopreventive modality in the experimentally induced HBP SCC. The gross observation, histopathological findings and the DOI utilizing H&E stain and the histochemical results utilizing AgNOR stain and picrosiures red stain as proliferative and invasive marker respectively in addition to the statistical analysis results revealed variable interest.

The gross observation in GI (normal), all hamsters appeared active and healthy. The HBP mucosa has normal appearance (pink in color with smooth surface). Moreover, this finding reflected on H&E stain that showed the classical epithelium mucosal layer. This finding was in consistence with that of other studies^(28,29). With regard to AgNOR stain, currant study recorded the mean dots number per nucleus in GI was 2.1. This result is almost in agreement with that shown by other investigators (1.5)^(30,31). **Buddhdev et al (2017)**⁽³²⁾ suggested that

these results could be attributed to in normal cells, the AgNOR protein are tightly packed in nucleoli and are indiscernible.

In the present study, the picrosiures red stain results in GI recorded the mean area fraction of collagen fibers results was 43.8 %, while the mean area % of collagen type I (reddish-orange birefringence) 90% and the mean area % collagen type III (greenish-yellow birefringence) 10%. These results are in agreement with that shown by other investigators (40.2%)^(19,33). These results could be attributed to during maturation of collagen fibers, there is change in proteoglycan content of fibers causing dehydration of fibers resulting in increases the number of cross-links and stainable side groups; thus the diameter of collagen fibers grows markedly and increase the intensity of birefringence. Hence, the change in polarizing colors. Thus young, very fine type I collagen fibers with weak birefringence appear green in color similar to the mature type III fibers. They become orange or red in the further maturative stage⁽³⁴⁾.

In the current study, the gross observation results in GII (DMBA treated group) at 14 weeks, all hamsters appeared loss of activity and also debilitation. The right HBP mucosa revealed exophytic tumor growth of variable sizes surrounded with hemorrhagic and ulcerative areas. This result was confirmed by the H&E stain which indicated that, the overlying epithelium revealed multiple areas of dysplastic features accompanied with destructive basement membrane and provided evidence of prominent true invasion with development of invasive SCC (well and moderately differentiated) similar those have been seen in human oral carcinoma⁽³⁵⁾. This result of HBP provided a useful system upon which to evaluate structure alterations by different investigations during carcinoma induction by DMBA⁽³⁶⁾. In the current study, the mean depth of invasion result was seen between the muscle fiber (7mm). This result is in consistence with those of other studies⁽³⁷⁻³⁹⁾. **Van Lanschot et al (2020)**⁽³⁷⁾ reported that the aggressiveness of tumor characteristics

including tumor differentiation grades associated with deeper invasion when it becomes more than 4mm). This is in consistence with that shown by other studies^(40,41). HBP SCC result is due to repeated exposure of carcinogens to the entire epithelial cells of the HBP. Phase I enzymes are involved in the metabolic activation of carcinogenic agents, phase II enzymes are involved in the detoxification of carcinogenic agents, the activities of phase I enzymes were increased, whereas, phase II detoxification agents were decreased in the liver of hamsters painted with DMBA alone, thus suggested that the carcinogenic metabolite of DMBA, dihydrodiol epoxide, was excessive metabolic activation of DMBA, which impaired the activities of phase II detoxification agents. Buccal mucosa phase I and II detoxification agents were significantly increased in hamsters treated with DMBA alone. Extensive studies reported that increase in the activities of phase I and II enzymes was probably due to repeated carcinogenic exposure in the buccal mucosa^(42,43). The present results supported the concept that DMBA induced HBP carcinoma appear to go through the same changes as in human at the gross observations as well as on histopathological alteration results. These results are in concurrence with those of other studies⁽⁴⁴⁻⁴⁶⁾.

Regarding the AgNOR stain, there was high significant difference between GII and GI with p value < 0.001. This result is in agreement with that reported by other studies^(30,31). **Williams et al (2018)**⁽³⁰⁾ demonstrated that the increase the mean AgNOR dots number can be explained as result of increase the number of chromosomes and mitotic activity in malignant cells. These observations might be attributed to DMBA effect on metabolic activation. DMBA is converted into its active carcinogenic metabolite, dihydrodiol epoxide, which mediates carcinogenesis through chronic inflammation, overproduction of ROS, activation of protooncogene, inactivation of tumor suppressor genes, extensive DNA damage and reduction in DNA damage repair which reduced the ability to induce apoptosis^(44,47).

Regarding the picrosures red stain, the area fraction of the collagen fibers recorded high significant difference between GII and GI with p value < 0.001. Also, the polarizing colors of collagen fibers recorded significant difference between GII and GI with p values: 0.042. This result is in agreement with that of other studies^(19,33). This result could be attributed to the action of enzymatic degradation such as collagenases or metalloproteinase on the existing collagenase stroma that lead to increase the amount of collagen type III which occurs singly rather than in bundles like collagen type I or due to the formation of new abnormal/pathologic collagen by tumor cells⁽²⁷⁾.

In the present study, the hamsters general healthy condition results in GIII (honokiol chemopreventive group), showed improvements in 6 out of 10 (they were almost healthy and active) compared to GII. The right HBP mucosa showed a relatively less extensive tumor growth, ulcerative and bleeding areas compared to GII. H&E stain confirmed these improvements and revealed that the changes are limited to the epithelial layer in the form of (hyperplastic epithelium with no features of epithelial dysplasia, moderate epithelial dysplasia, and severe epithelial dysplasia) while the basement membrane appeared intact with no evidence of true invasion or nest formation. The gross observations of other 4 hamsters revealed, almost, the same observations of GII and these results were confirmed by H&E stain which indicated that, the overlying epithelium had obvious dysplastic features accompanied destruction of the basement membrane and the underlying connective tissue contained superficial invasive epithelial nests and keratin pearl (DOI : less than 4mm). While the mean depth of invasion results of GIII revealed high significant difference compared to that of GII with p value < 0.001. This result is in agreement with that reported by **Wang et al (2017)**⁽⁴⁸⁾ who suggested that honokiol may play important role in restored the depleted non-enzymatic antioxidants due to its potent free radical scavenging activity.

Regarding the AgNOR stain there was high significant difference between GIII and GII with p value < 0.001. These results are in agreement with those of other studies^(49,50). **Huang et al (2018)**⁽⁴⁹⁾ suggested that these results could be attributed to the role of honokiol in retards cell cycle at G1 stage, by downregulation of cyclin D1 and cyclin-dependent kinases (Cdk2 and Cdk4) and upregulation of cell cycle suppressors Cdk inhibitors, p21 and p27.

Regarding the picrosures red stain, the area fraction of the collagen fibers recorded high significant difference between GIII and GII with p value < 0.001. Also, the polarizing colors of collagen fibers recorded significant difference between GIII and GII with p value: 0.175. These results are in consistency with those of other studies^(51,52). These results could be attributed to the role of honokiol in activation of Adenosine 5'-phosphate-activated protein kinase (AMPK) pathway that lead to down regulation of mTOR pathway, which regulated cell invasion and migration by regulating MMP9⁽⁵¹⁾.

Correlation between proliferation and invasion:

From the present study, there was a significant positive (direct) correlation among mean AgNOR dots number per nucleus and mean depth of invasion with p value < 0.001. This means that an increase one variable is associated with in the increase other variable and vice versa. The mean AgNOR dots number per nucleus and mean depth of invasion showed statistically significant negative (revers) correlation with mean area of fraction of collagen fiber with p value 0.001. This means that an increase in both variable is associated with decrease in the other variable and vice versa. These results could be attributed to that highly proliferative tumors could initiate invasive behavior non-cell autonomously by recruiting stromal cells to facilitate dissemination and intravasation⁽⁵³⁻⁵⁵⁾. The majority of cancer literature assumed a positive correlation between cell proliferation and cell invasive activ-

ity⁽⁵⁶⁾. This indicated that proliferation is linked with increased invasion^(57,58).

The present study demonstrated that honokiol significantly inhibited the proliferation and invasion potentially of cancer cells compared to DMBA treated group with p value < 0.001. These results could be attributed to the role of honokiol in activities potentially of cancer cells through activation of AMPK pathway that lead to down regulation of mTOR pathway, which regulates apoptosis, cell growth, migration and invasion. The mTOR pathway inhibits apoptosis via the regulation of the tumor suppressors p27 and p53. The mTOR/4EBP1 pathway regulates cell invasion and migration by regulating MMP-9⁽⁵¹⁾.

CONCLUSION

From the results of the present study the following conclusions could be drawn:

1. The depth of invasion of tumor cells was a significant for tumor progression in DMBA induced HBP SCC as shown by H&E stain.
2. The proliferative activity of tumor cells was a significant for tumor progression in DMBA induced HBP SCC as shown by AgNOR stain.
3. The area fraction and the polarizing colors of collagen fibers were a significantly for tumor progression in DMBA induced HBP SCC as shown by picrosures red stain.
4. Honokiol significantly inhibited the DOI of tumor cells in DMBA induced HBP SCC as shown by H&E stain.
5. Honokiol significantly inhibited the proliferative activity of tumor cells in DMBA induced HBP SCC as shown by AgNOR stain.
6. Honokiol significantly increase the area fraction and the polarized colors of collagen fibers, which in turn inhibited invasion as shown by picrosures red stain.

REFERENCE

1. Ng J, Iyer N, Tan M, Edgren G. Changing epidemiology of oral squamous cell carcinoma of the tongue: A global study *Head Neck* 2017; 39: 297-304.
2. Du M, Nair R, Jamieson L, Liu Z, Bi P. Incidence trends of lip, oral cavity, and pharyngeal cancers: global burden of disease 1990-2017. *J Dent Res* 2020; 99(2): 143-51.
3. Manoharan S, Silvan S, Vasudevana K, Baskaran N, Kumar S, Vinoth K, et al. Carnosic acid, a potent chemopreventive agent in oral carcinogenesis. *Chem Biol Interact* 2010; 188: 616-22.
4. Neville B, Day T. Oral cancer and precancerous lesions. CA. *Cancer J. Clin* 2002; 52:195-215.
5. Furness S, Glennly A, Worthington H, Pavitt S, Oliver R, Clarkson J, et al. Interventions for the treatment of oral cavity and oropharyngeal cancer: chemotherapy. *Cochrane Database Syst Rev* 2010; (9): CD006386.
6. Li S, Kuo H, Yin R, Wu R, Liu X, Wang L, et al. Epigenetics/epigenomics of triterpenoids in cancer prevention and in health. *Biochem. Pharmacol* 2020; 175: 113890.
7. Arora I, Sharma M, Tollefsbol T. Combinatorial epigenetics impact of polyphenols and phytochemicals in cancer prevention and therapy. *Int. J. Mol. Sci* 2019; 20: 1- 47.
8. Sarrica A, Kirika N, Romeo M, Salmona M, Diomedea L. Safety and toxicology of magnolol and honokiol. *Planta Med* 2018; 84: 1151-64.
9. Ong C, Lee W, Tang Y, Yap W. Honokiol: a review of its anticancer potential and mechanisms. *Cancers* 2019; 12: 48.
10. Derenzini M, Thiry M, Gessens G. Ultrastructural cytochemistry of the mammalian cell nucleolus. *J Histochem Cytochem* 1990; 38:1237-1256.
11. Derenzini M, Ploton D. Interphase nucleolar organizer region in cancer cell. *Int Rev EXP Pathol* 1991; 32: 149-92.
12. Venigella A, Charu S. Evaluation of collagen in different grades of oral squamous cell carcinoma by using the picrosirius red stain: a histochemical study. *J Clin Diagn Res* 2010; 4: 3444-49.
13. Conti J, Thomas G. The role of tumor stroma in colorectal cancer invasion and metastasis. *Cancers* 2011; 3: 2160-68.
14. Berdugo J, Thompson L, Purgina, B, Sturgis C, Tuluc M, Seethala R, et al. Measuring depth of invasion in early squamous cell carcinoma of the oral tongue: positive deep margin, extratumoral perineural invasion and other challenges. *Head and Neck Pathology* 2019; 13:154-61.
15. Amin M, Edge S, Greene F, Byrd D, Brookland R, Washington M. et al. *AJCC Cancer Staging Manual*, 8th ed. Springer International Publishing 2017; 67(2): 93-99.
16. Rich L, Whittaker P. Collagen and picrosirius red staining. A polarized light assessment of fibrillar hue and spatial distribution. *Braz J Morphol Sci* 2005; 22: 997-1004.
17. Rich L, Whittaker P, Picrosirius R. A polarized light assessment of fibrillar hue and spatial distribution. *Braz J Morphol Sci* 2005; 22: 97-104.
18. Rose M, Everitt J, Hedrich H, Schofield J, Dennis M, Scott E, et al. ICLAS working group on harmonization: international guidance concerning the production care and use of genetically-altered animals. *Lab Anim* 2013; 47(3):146-52.
19. Kullage S, Jose M, Shanbhag V, Abdulla R. Qualitative analysis of connective tissue stroma in different grades of oral squamous cell carcinoma: A histochemical study. *Indian J Dent Res* 2017; 28(4): 355-61.
20. Vinoth A, Kowsalya R. Chemopreventive potential of vanillic acid against 7,12-dimethylbenz(a)anthracene-induced hamster buccal pouch carcinogenesis. *J Cancer Res Ther* 2018; 14(6): 1285-90.
21. Khalid S, Ullah M, Khan A, Afridi R, Rasheed H, Khan A, et al. Antihyperalgesic properties of honokiol in inflammatory pain models by targeting of NF- κ B and Nrf2 signaling. *Front Pharmacol* 2018; 26(4): 1037-49.
22. Berdugo J, Thompson L, Purgina, B, Sturgis C, Tuluc M, Seethala R, et al. Measuring depth of invasion in early squamous cell carcinoma of the oral tongue: positive deep margin, extratumoral perineural invasion and other challenges. *Head and Neck Pathology* 2019; 13: 154-61.
23. Ploton D, Menager M, Jeannesson P, Himer G, Pigeon F, Adnet J, et al. Improvement on the staining and in the visualization of the argyrophilic proteins of the nucleolar organizer region at the optical level. *Histochem J* 1986; 18: 5-14.
24. Crocker J, Boldy D, Egan M. How should we count Ag-NOR's? Proposals for a standardized approach. *J Pathol* 1989; 158: 185-88.
25. Junqueira L, Bignolas G, Brentani R. Picrosirius staining plus polarization microscopy, a specific method for collagen detection in tissue sections. *Histochem J* 1979; 11: 447-55.
26. Venigella A, Charu S. Evaluation of collagen in different grades of oral squamous cell carcinoma by using the picrosirius red stain: A histochemical study. *J Clin Diagn Res* 2010; 4: 3444-49.

27. Kardam P, Mehendiratta M, Rehani S, Kumra M, Sahay K, Jain K. Stromal fibers in oral squamous cell carcinoma: a possible new prognostic indicator? *J Oral Maxillofac Pathol* 2016; 20: 405-12.
28. Kathiresan S, Mariadoss A, Muthusamy R, Kathiresan S. [6]-Shogaol, a novel chemopreventor in 7, 12-Dimethylbenz[a] anthracene-induced hamster buccal pouch carcinogenesis. *Phytother Res* 2016; 30(4): 646-53.
29. Li Y, Zheng Y, Wang Huibo. Anticancer activity of Vicenin-2 against 7,12 dimethylbenz[a]anthracene-induced buccal pouch carcinoma in hamsters. *Biochemical and Molecular Toxicology* 2020; 35(3): e22673.
30. Williams K, Gideon A, Yanhui A, Kwabena O, Ernest A. Assessment of proliferative index in different grades of breast cancers using AgNOR (Agyrophilic Nuclear Organizer Region) expression. *Journal of Basic and Applied Sciences* 2018; 7(4): 587-92.
31. Moradzadeh Khiavi M, Vosoughhosseini S, Halimi M, Mahmoudi S, Yarahmadi A. Nucleolar organizer regions in oral squamous cell carcinoma. *J Dent Res Dent Clin Dent Prospects* 2012; 6(1): 17-20.
32. Buddhdev P, Monali C, Hemant K, Malay B, Tapan M. Quantitative and qualitative assessment of argyrophilic nucleolar organizer regions in normal, premalignant and malignant oral lesions. *J Oral Maxillofac Pathol* 2017; 21(3): 360-66.
33. Aeman K, Safia S, Bharadwaj B, Nafis F, Fahad S, Noora S. An immunohistochemical and polarizing microscopic study of the tumor microenvironment in varying grades of oral squamous cell carcinoma. *J Pathol Transl Med* 2018; 52(5): 314-22.
34. Szendrői M, Vajta G, Kovács L, Schaff Z, Lapis K. Polarization colors of collagen fibers: A sign of collagen production activity in fibrotic processes. *Acta Morphol Hung* 1984; 32: 47-55.
35. Sowmya S, Rao R, Prasad K. Development of clinicohistopathological predictive model for the assessment of metastatic risk of oral squamous cell carcinoma. *J Carcinog* 2020, 19: 16-19.
36. Martínez B, Barato Gómez P, Iregui Castro C, Rosas Pérez J. DMBA-induced oral carcinoma in syrian hamster: increased carcinogenic effect by dexamethasone coexposure. *Biomed Res Int* 2020; 2020: 1470868.
37. Van Lanschot C, Klazen Y, de Ridder M, Mast H, Ten Hove I, et al. Depth of invasion in early stage oral cavity squamous cell carcinoma: The optimal cut-off value for elective neck dissection. *Oral Oncol* 2020; 111: 104940.
38. Masood M, Farquhar D, Vanleer J, Patel S, Hackman T. Depth of invasion on pathological outcomes in clinical low-stage oral tongue cancer patients. *Oral Dis* 2018; 24(7): 1198-1203.
39. Hans C, Brockhoff D, Roderick Y, Kim D, Thomas M, et al. Correlating the depth of invasion at specific anatomic locations with the risk for regional metastatic disease to lymph nodes in the neck for oral squamous cell carcinoma 2017; 39(5): 974-79.
40. Vinoth A, Kowsalya R. Chemopreventive potential of vanillic acid against 7,12-dimethylbenz(a)anthracene-induced hamster buccal pouch carcinogenesis. *J Can Res Ther* 2018; 14: 1285-90.
41. Periyannan V, Veerasamy V. Syringic acid may attenuate the oral mucosal carcinogenesis via improving cell surface glycoconjugation and modifying cytokeratin expression. *Toxicology Reports* 2018; 5: 1098-1106.
42. Karthikeyan S, Srinivasan R, Wani S, Manoharan S. Chemopreventive potential of chrysin in 7,12-dimethylbenz(a) anthracene induced hamster buccal pouch carcinogenesis. *Int J Nutr Pharmacol Neurol Dis* 2013; 3: 46-53.
43. Manoharan S, Balakrishnan S, Menon V, Alias L, Reena A. Chemo-preventive efficacy of curcumin and piperine during 7,12dimethylbenz[a]anthracene induced hamster buccal pouch carcinogenesis. *Singapore Med J* 2009; 50: 139-46.
44. Manoharan S, Wani S, Vasudevan K. Saffron reduction of 7, 12-dimethylbenz[a]anthracene-induced hamster buccal pouch carcinogenesis. *Asian Pac J Cancer Prev* 2013; 14: 951-57.
45. Nagini S, Letchoumy P, Thangavelu A, Ramachandran C. A comparative evaluation of carcinogen activation, DNA damage, cell proliferation, apoptosis, invasion and angiogenesis in oral cancer patients and hamster buccal pouch carcinomas. *Oral Oncol* 2009; 45: 31-37.
46. Silvan S, Manoharan S. Apigenin prevents deregulation in the expression pattern of cell-proliferative, apoptotic, inflammatory and angiogenic markers during 7, 12-dimethylbenz (a) anthracene-induced hamster buccal pouch carcinogenesis. *Arch Oral Biol* 2013; 58: 94-101.
47. Murata M, Ohnishi S, Seike K, Fukuhara K, Miyata N, Kawanishi S, et al. Oxidative DNA damage induced by carcinogenic dinitropyrenes in the presence of P450 reductase. *Chem Res Toxicol* 2004; 17(12):1750-56.
48. Wang Z, Zhang X. Chemopreventive Activity of honokiol against 7, 12 - Dimethylbenz[a]anthracene-induced mammary cancer in female sprague dawley rats. *Front Pharmacol* 2017; 8: 1-11.

49. Huang K, Kuo C, Chen S, Lin C, Lee Y. Honokiol inhibits in vitro and in vivo growth of oral squamous cell carcinoma through induction of apoptosis, cell cycle arrest and autophagy. *J Cell Mol Med* 2018; 22(3): 1894-1908.
50. Li Z, Dong H, Li M, Wu Y, Liu Y, Zhao Y, et al. Honokiol induces autophagy and apoptosis of osteosarcoma through PI3K/Akt/mTOR signaling pathway. *Mol Med Rep* 2018; 17(2): 2719-23.
51. Lee J, Sul J, Park J, Lee M, Cha E, Ko Y, et al. Honokiol induces apoptosis and suppresses migration and invasion of ovarian carcinoma cells via AMPK/mTOR signaling pathway. *Int J Mol Med* 2019; 43(5): 1969-78.
52. Singh T, Katiyar S. Honokiol inhibits non-small cell lung cancer cell migration by targeting PGE2-mediated activation of β -Catenin signaling. *PLoS ONE* 2013; 8: e60749.
53. Gaggioli C. Collective invasion of carcinoma cells: when the fibroblasts take the lead. *Cell adhesion & migration* 2008; 2: 45-47.
54. Harney A, Arwert E, Entenberg D, Wang Y, Guo P, Qian B, et al. Real-time imaging reveals local, transient vascular permeability, and tumor cell intravasation stimulated by tIE2hi macrophage-derived VEGFA. *Cancer Discov* 2015; 5:932-43.
55. Gaggioli C, Hooper S, Hidalgo-Carcedo C, Grosse R, Marshall J, Harrington K, et al. Fibroblast-led collective invasion of carcinoma cells with differing roles for RhoGTPases in leading and following cells. *Nat Cell Biol*. 2007; 9:1392-1400.
56. Kohrman A, Matus D. Divide or conquer: cell cycle regulation of invasive behavior. *Trends Cell Biol* 2017; 27(1):12-25.
57. Tumuluri V, Thoma G, Fraser I. The relationship of proliferating cell density at the invasive tumour front with prognostic and risk factors in human oral squamous cell carcinoma. *J Oral Pathol Med* 2004; 33: 204-208.
58. Dissanayake U, Johnson N, Warnakulasuriya K. Comparison of cell proliferation in the centre and advancing fronts of oral squamous cell carcinomas using Ki-67 index. *Cell Prolif* 2003; 36: 255-64.